Progress In Electromagnetics Research Letters, Vol. 98, 129–137, 2021

Analysis and Design of Miniaturized Wideband Rat-Race Coupler with Improved Phase Performance

Hongmei Liu*, Yao Wang, Tielin Zhang, Shaojun Fang, and Zhongbao Wang

Abstract—In the paper, a miniaturized wideband rat-race coupler with improved phase performance is designed and analyzed. Flat output ports phase differences are obtained by utilizing a component-loaded T-type transmission line (CLT-TL) with a stub-loaded short-circuited coupled line (SLS-CL). Let the CLT-TL and SLS-CL sections be equivalent to uniform 90° and 270° transmission lines, respectively. Design equations are derived, and an optimization is proceeded to obtain the circuit parameters. For validation, a prototype is designed, fabricated, and measured. Including the feeding lines, the circuit size is $0.31\lambda_g \times 0.31\lambda_g$. Under the criterion of return loss (RL) > 10 dB, the measured bandwidths for ports 1 and 3 excitations are both 48%. For amplitude imbalance (AP) < 0.5 dB, the overlap relative bandwidth is 46.88%. The measured bandwidths with 2° phase imbalance are 49.58% and 54.01% for ports 1 and 3 excitations, respectively.

1. INTRODUCTION

Rat-race couplers are a fundamental component in RF and microwave front ends (e.g., mixers, push/pull amplifiers, phase shifters, and feeding networks of antenna arrays), offering the ability to be used as an in-phase or out-of-phase combiner. However, since a traditional rat-race coupler is composed of three $\lambda/4$- and one $3\lambda/4$-line sections, it exhibits the well-known drawbacks of large size and narrow bandwidth [1]. Thus, several researches have been focused on the size reduction and bandwidth enhancement of the rat-race coupler in the past decades.

For microstrip line, slow-wave structures have been extensively studied to reduce the circuit size [2–5]. The mechanism behind slow-wave propagation is to separately store electric and magnetic energies as much as possible in guided-wave media. Although obvious size reduction is obtained, the complexity of the circuit structure is increased. By using high-impedance T-equivalent structures to replace the conventional transmission lines, significant circuit size reduction can also be implemented [6]. However, it leads to the obvious degradation of the impedance matching and phase-difference bandwidths. To enhance the bandwidth, asymmetrical T-structures composed of a low-impedance shunt stub and two series high-impedance lines with unequal electrical lengths are presented [7]. A size reduction of 12.2% is realized with a bandwidth of 35.5%. But modifications are added when the asymmetric structure is used as a replacement. The symmetric equivalent circuits include lumped-element models [8], T-type [9, 10], and Π-type [11]. Using the T-type and Π-type sections, the rat-race coupler may be reduced, but the performance of the resulting coupler is worse than that of the original ones, and so do the ones with lumped element models.

For bandwidth enhancement, the coupled-line structures [12–14] have been widely studied in recent years. However, very small gaps between the coupled lines are required, and due to that the coupling between the edges of the coupled-lines is based on the fringing fields, which results in manufacturing difficulty. To increase the gap, several effective methods have been proposed, for instance, using

Received 6 May 2021, Accepted 11 June 2021, Scheduled 28 June 2021
* Corresponding author: Hongmei Liu (lhm323@dlmu.edu.cn).
The authors are with the School of Information Science and Technology, Dalian Maritime University, Dalian, Liaoning 116026, China.

defected ground structure [15], broadside-coupled striplines [16], and vertical installed planar (VIP) technique [17].

Except reducing the circuit size and widening the impedance bandwidth, the phase performance of the rat-race coupler is another important index, especially in the applications of the antenna feeding networks and phase shifters. However, few approaches have been proposed for increasing the phase performance. In the reported literatures, the common phase imbalance in the operation bandwidth is 5°.

In the paper, a miniaturized wideband rat-race coupler with improved phase performance is proposed. The 90° transmission lines (TLs) and 270° TL of conventional rat-race coupler are replaced by component-loaded T-type transmission lines (CLT-TLs) and the stub-loaded short-circuited coupled line (SLS-CL), respectively, to obtain a wide bandwidth and flat output ports phase differences. For demonstration, a prototype is designed and measured. The measured results are in good agreement with the simulated ones.

2. THEORETICAL ANALYSIS

Figure 1 shows the schematic of the proposed rat-race coupler with flat phase performance. It is composed of three sections of CLT-TL and one SLS-CL. The CLT-TL consists of two pairs of inductor/capacitor-loaded shunt stubs and a T-type transmission line with the period of 3. The inductor/capacitor-loaded shunt stub has a characteristic impedance of Z_o and an electrical length of θ_o. Let L_1 be the inductance of the inductor and C_1 be the capacitance of the capacitor. Each cell of the T-type transmission line is composed of two transmission lines (electrical length of θ_1 and characteristic impedance of Z_1) and one open stub (electrical length of θ_2 and characteristic impedance of Z_2).

The SLS-CL consists of two-end short-circuited coupled lines and two pairs of open-stub loaded

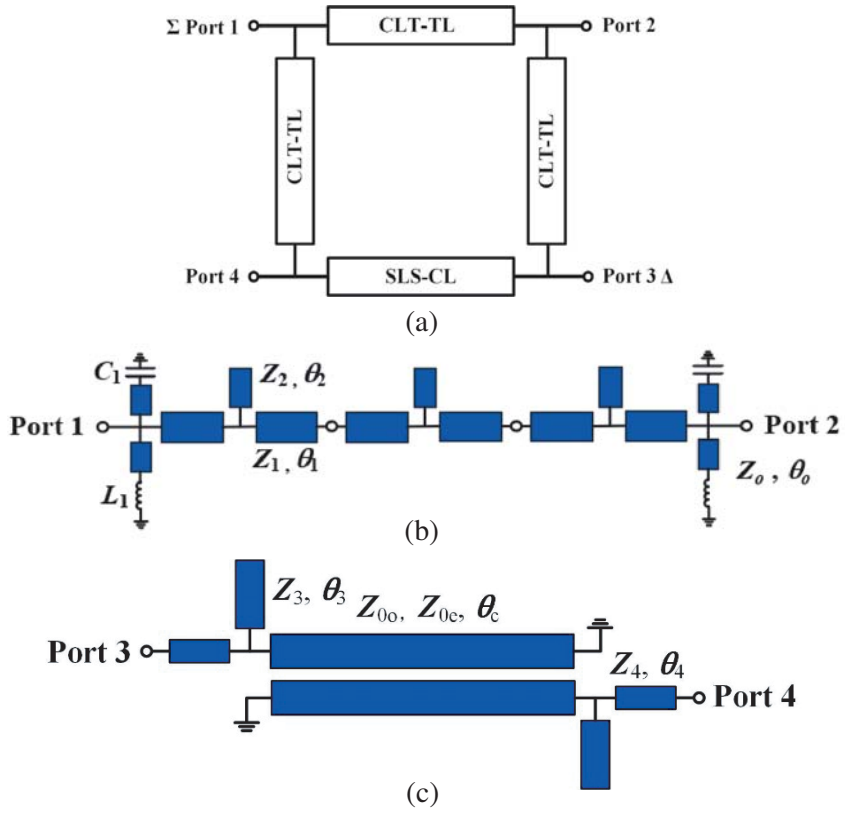

Figure 1. Schematic of (a) the proposed rat-race coupler, (b) CLT-TL, and (c) SLS-CL.

transmission lines. The even- and odd-mode characteristic impedances of the coupled line with θ_c long are defined as Z_o and Z_e, respectively. The characteristic impedances of the open stub and the transmission line are Z_3 and Z_4, and the electrical lengths are θ_3 and θ_4, respectively.

According to the circuits shown in Figures 1(b) and (c), the S-parameters of the CLT-TL and SLS-CL can be obtained, as shown in Eq. (1). And the phase difference between the CLT-TL and SLS-CL sections can be expressed as Eq. (2). Detailed derivations and expressions of parameters A_C, B_C, C_C, A_T, B_T, and C_T can be found in the appendix.

$$S_{11} = S_{22} = \left(\frac{B_T}{Z_0} - C_T Z_0\right) \Big/ \left(2A_T + \frac{B_T}{Z_0} + C_T Z_0\right) \tag{1a}$$

$$S_{33} = S_{44} = \left(\frac{B_C}{Z_0} - C_C Z_0\right) \Big/ \left(2A_C + \frac{B_C}{Z_0} + C_C Z_0\right) \tag{1b}$$

$$S_{12} = S_{21} = \frac{2}{2A_T + B_T/Z_0 + C_T Z_0} \tag{1c}$$

$$S_{34} = S_{43} = \frac{2}{2A_C + B_C/Z_0 + C_C Z_0} \tag{1d}$$

$$\Delta\phi = \tan^{-1}\left(\frac{\frac{B_C}{Z_0} + C_C Z_0}{-\mathrm{j}\frac{B_C}{2A_C}}\right) - \tan^{-1}\left(\frac{\frac{B_T}{Z_0} + C_T Z_0}{-\mathrm{j}\frac{B_T}{2A_T}}\right) \tag{2}$$

Here, Z_0 is the port impedance in the CLT-TL and SLS-CL sections. In the design, the value of Z_0 for the CLT-TL and SLS-CL sections is assigned as $70.71\,\Omega$ after considering the characteristic impedance of each transmission line section in the traditional rat-race coupler.

According to design requirements for a rat-race coupler, the conditions of Eq. (3) should be satisfied

$$S_{11}(f_i) = S_{22}(f_i) = S_{33}(f_i) = S_{44}(f_i) = 0 \arg(S_{21}(f_0)) = -90^\circ \arg(S_{43}(f_0)) = -270^\circ \Delta\phi(f_i) = 180^\circ \tag{3a}$$

$$f_i = f_0\left(1 + \frac{i-1}{D}\right) \quad (i = 1, \ldots\ldots, N) \tag{3b}$$

Here, N is the number of sampling points, f_0 the center frequency, f_i the sampling frequency, and f_0/D the sampling interval. Based on Eq. (3), an objective function F can be defined [19], as listed in Eq. (4).

$$F = \sum_{i=1}^{N} |S_{11}(f_i)|^2 + \sum_{i=1}^{N} |S_{33}(f_i)|^2 + |\arg(S_{21}(f_0)) + 90^\circ|^2 + |\arg(S_{43}(f_0)) + 270^\circ|^2 + \sum_{i=1}^{N} |\Delta\phi(f_i) - 180^\circ|^2 \tag{4}$$

It is noted that since the characteristics of the rat-race coupler within the operation band can be approximately considered as symmetrical corresponding to the center frequency f_0, only half of the frequency band is calculated in the optimization. By minimizing the objective function F using the particle swarm optimization [20], the circuit parameters of the coupler can be obtained. To simplify the optimization process, specific tolerance limits can be assigned according to the required performance, as shown in Eq. (5).

$$S_{11}(f_i) = S_{33}(f_i) < -15\,\mathrm{dB} \tag{5a}$$

$$|\arg(S_{21}(f_0)) + 90^\circ| < 2^\circ \tag{5b}$$

$$|\arg(S_{43}(f_0)) + 270^\circ| < 2^\circ \tag{5c}$$

$$|\Delta\phi(f_i) - 180^\circ| < 2^\circ \tag{5d}$$

Besides, considering the widths of transmission lines, the ranges of Z_1, Z_2, Z_3, and Z_4 are fixed from $60\,\Omega$ to $90\,\Omega$. In order to obtain a compact circuit size, the values of θ_1 and θ_2 are determined to be greater than 5° and less than 15°, and the value of θ_c should be less than 60°. With all limitations, groups of parameters can be calculated by using the particle swarm optimization.

3. IMPLEMENTATION AND RESULTS

In this section, a prototype is designed at the center frequency of 1.4 GHz to validate the derived equations. According to the target relative bandwidth of 40%, the edge frequencies are 1.12 GHz and 1.68 GHz. In the objective function, the sampling points N is selected as 9, and the corresponding sampling interval f_0/D is 0.035 GHz with $D = 40$. Table 1 shows one group of the calculated parameters. Figure 2 shows the calculated results according to the design parameters. It is observed that under the criterion of $|S_{11}| = |S_{33}| < -10$ dB, the relative bandwidth is from 1.06 GHz to 1.73 GHz. The in-band isolations are both larger than 35 dB. For amplitude imbalance < 0.5 dB, the bandwidth for ports 1 and 3 excitations are 85.7% and 73%, respectively. For port 1 excitation, the relative bandwidth for output ports phase differences (PD) $< 2^\circ$ is 84%. The same bandwidth (PD $< 2^\circ$) is also obtained for port 3 excitation.

Table 1. One group of the calculated parameters.

C (pF)	Z_o (Ω)	Z_1 (Ω)	Z_2 (Ω)	Z_3 (Ω)	Z_4 (Ω)	Z_o (Ω)	Z_e (Ω)
0.6	156	72.6	76.6	81.7	76.1	27.1	130.4
L (nH)	θ_o ($^\circ$)	θ_1 ($^\circ$)	θ_2 ($^\circ$)	θ_3 ($^\circ$)	θ_4 ($^\circ$)	θ_c ($^\circ$)	
11	1	13	8.7	4.7	38.9	58.4	

Using an F4B substrate ($\varepsilon_r = 3.5$, $\tan\delta = 0.003$, $h = 1.5$ mm), a prototype was fabricated. Figure 3(a) shows the layout of the designed circuit. Based on the calculated parameters, the prototype is optimized using the Ansoft HFSS, and the final dimensions are listed in Table 2. To achieve tight coupling between the coupled lines, a VIP structure is applied. Since the space for the shunt stubs is limited, a component-loaded stub with halved characteristic impedance, halved inductance value, and doubled capacitance value is served as a replacement. A similar method is also applied at the points with four stubs. Figure 3(b) shows a photograph of the fabricated coupler. The overall size of the coupler is 36 mm $\times$ 36 mm, corresponding to $0.31\lambda_g \times 0.31\lambda_g$. In the realization, two 1-pF (C_1) and two 2-pF (C_2) capacitors, two 18-nH (L_1) and two 9-nH (L_2) inductors are used.

Table 2. The optimized dimensions of the prototype (Unit: mm).

w_1	w_2	w_3	w_4	w_5	w_6	w_7	w_f	s	C_1	L_1	h_1
1.3	1.2	0.6	0.6	0.8	1.8	1.2	3.38	0.5	1 pF	18 nH	1.2
l_1	l_2	l_3	l_4	l_5	l_6	l_7	l_8	l_f	C_2	L_2	
8	2	20.6	1.7	13.6	2.2	3.2	2	6	2 pF	9 nH	

The fabricated prototype is measured using Agilent N5230A, and the measured results are plotted in Figure 4. It is observed that the measured results agree well with the simulated ones. When port 1 is excited, the bandwidth for 10-dB impedance matching is in the range of $1.08 \sim 1.78$ GHz (48.95%). Within the bandwidth, the isolation is more than 20 dB. For port 3 excitation, the bandwidth for $|S_{11}| < -10$ dB is from 1.1 GHz to 1.8 GHz (48.28%). Figures 4(b) and (c) show the output ports amplitude imbalance and phase differences of the fabricated rat-race coupler. Under the criterion of amplitude imbalance (AP) < 0.5 dB, the measured bandwidths for ports 1 and 3 excitations are 66.18% (0.92–1.83 GHz) and 46.88% (0.98–1.58 GHz). When the output ports phase differences (PDs) are in the range of $0^\circ/180^\circ \pm 2^\circ$, the measured bandwidths are $1.04 \sim 1.72$ GHz (49.58%) and $1 \sim 1.74$ GHz (54.01%), respectively. When the phase difference error is increased to 5°, the relative bandwidths are 76.92% and 79.7%, respectively. Table 3 shows the comparisons of the proposed rat-race coupler with related literatures. Compared with the rat race couplers in [6–9, 11, 12], the proposed rat-race coupler shows wider overlap bandwidth under the criterions of RL > 10 dB, AP < 0.5 dB, and PD $< 2^\circ$. Although the coupler in [2] exhibits wider bandwidth, the design of slow-wave structure is complicated, and dual-layer structures are used. Thus, the proposed structure can enhance the working frequency range in both matching and outputs, and achieve small size.

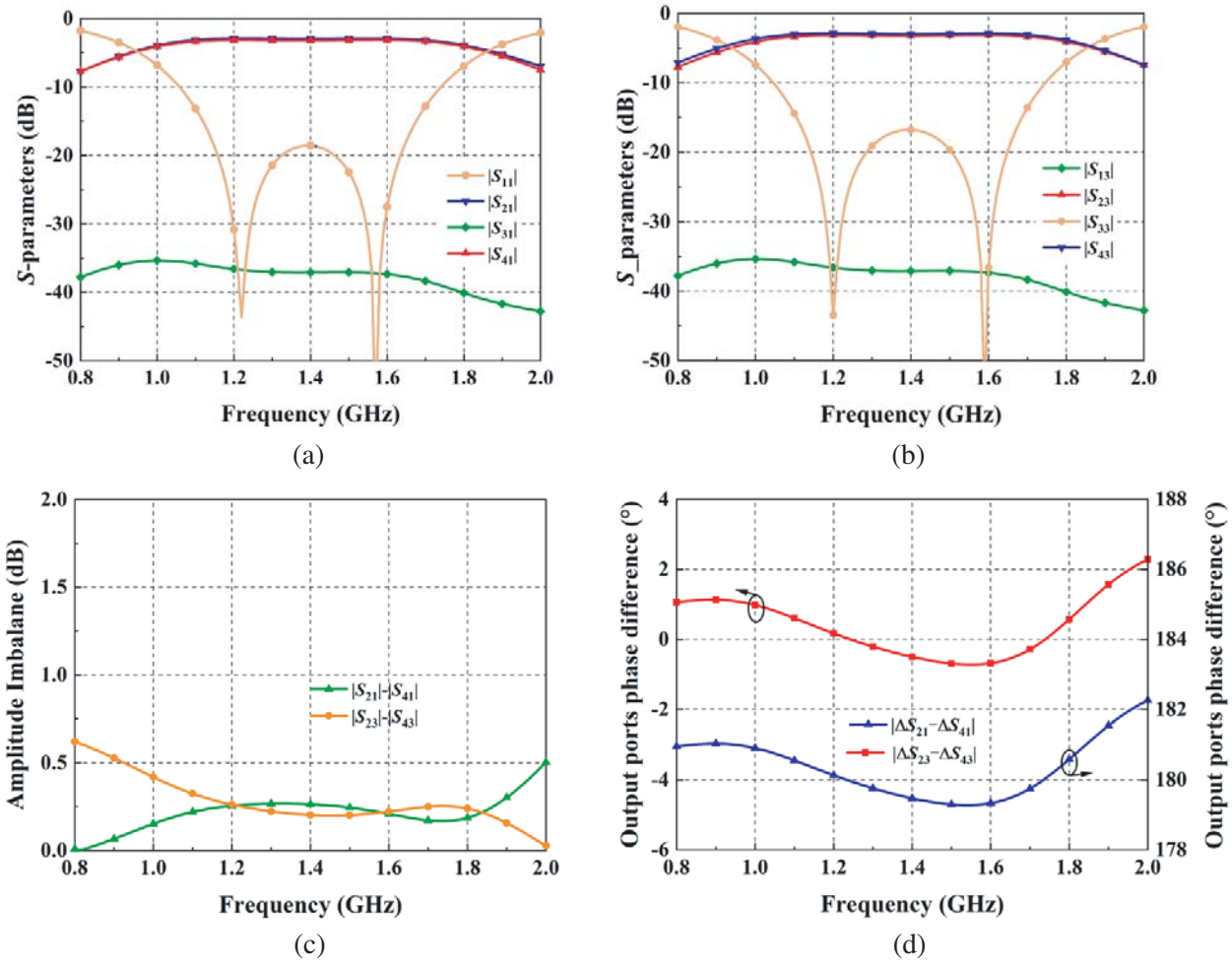

Figure 2. Calculated results of the proposed rat-race coupler. (a) S-parameters for port 1 excitation. (b) S-parameters for port 3 excitation. (c) Amplitude imbalance. (d) Output ports phase difference.

Table 3. Comparisons between the proposed rat-race coupler with related literatures.

Ref.	Technique	Relative Bandwidth(%)			Size ($\lambda_g \times \lambda_g$)
		$RL > 10$ dB	$AP < 0.5$ dB	$PD < 2°$	
Traditional	Transmission line	121.4/55.7	23.6/23.6	6.4/6.4	0.6×0.6
[2]	Slow-wave structure	61.1	57.5	57.5	0.09×0.09
[6]	The high-impedance T-equivalent structure	34.4	–	< 10	0.09×0.11
[7]	asymmetrical T-structure	35.5	< 36.7	< 36.7	0.08×0.13
[8]	lumped-element model	65	43/46	< 10	0.29×0.29
[9]	T-type model	55.6	< 27.8	< 22.2	0.16×0.45
[11]	II-type model	57.1	24.	< 8.2	0.46×0.46
[12]	the coupled-line structure	103.6	75	< 10	0.25×0.30
This work	**CLT-TL with SLS-CL**	**48.95/48.28**	**66.18/46.88**	**49.58/54.01**	0.31×0.31

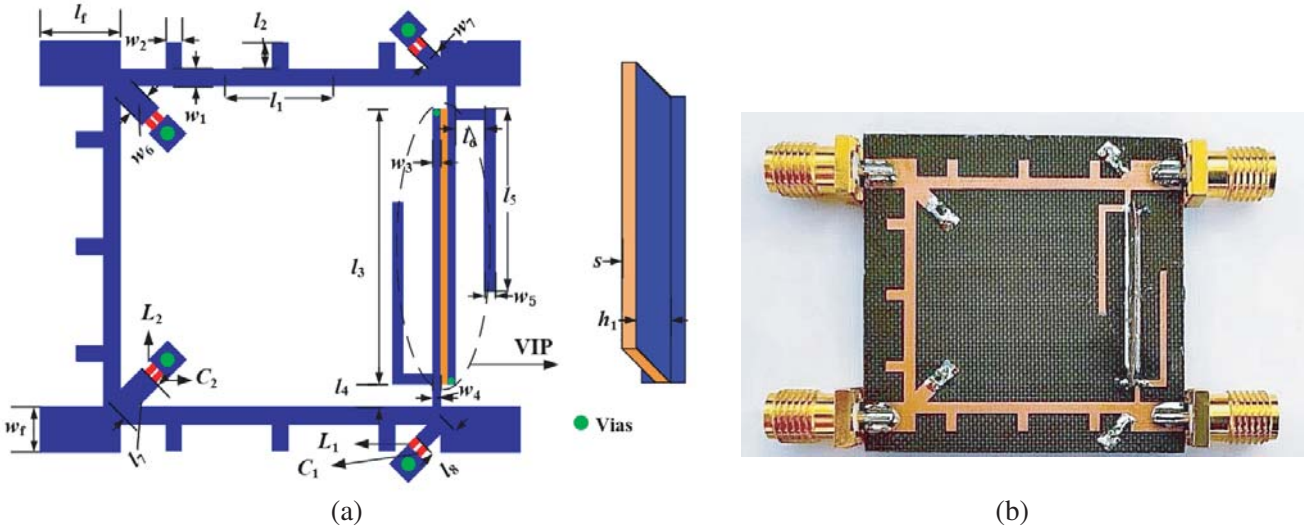

Figure 3. (a) The layout and (b) photograph of the rat-race coupler.

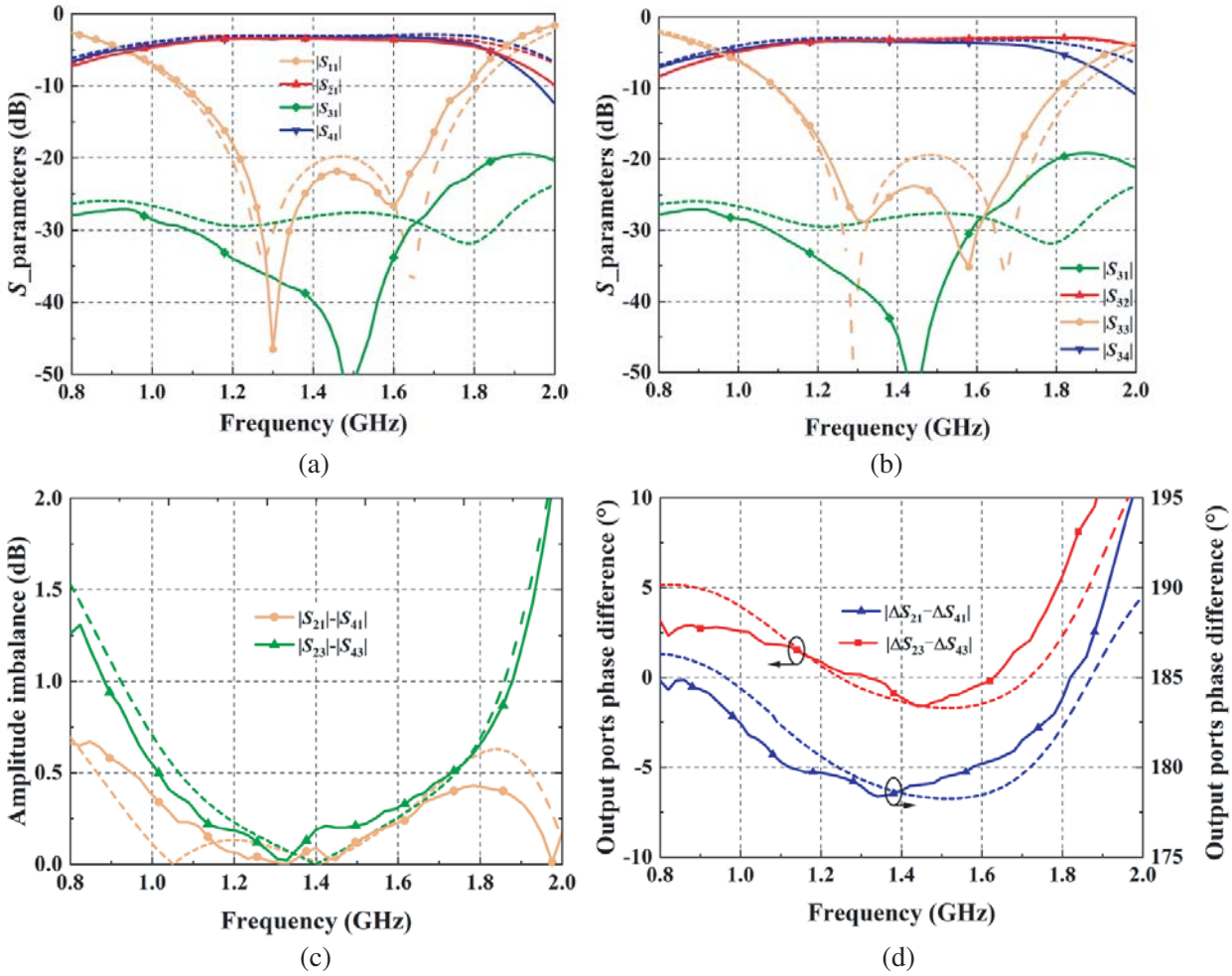

Figure 4. Simulated (dash line) and measured (solid line with symbol) results of the proposed rat-race coupler. (a) S-parameters for port 1 excitation. (b) S-parameters for port 3 excitation. (c) Amplitude imbalance. (d) Output ports phase difference.

4. CONCLUSION

In this paper, a miniaturized wideband rat-race coupler with improved phase performance is designed and analyzed. Based on the component-loaded T-type transmission line (CLT-TL) combined with the stub-loaded short-circuited coupled line (SLS-CL), flat output ports phase differences are obtained. For demonstration, a prototype with the dimension of $0.31\lambda_g \times 0.31\lambda_g$ is fabricated and measured. The overlap relative bandwidths for RL > 10 dB, AP < 0.5 dB, and PD $< 2^\circ$ are both larger than 45% for ports 1 and 3 excitations. The improvement in phase performance indicates that the proposed rat-race coupler is a good candidate for applications including phase shifters, mixers, and feeding networks of antenna arrays.

ACKNOWLEDGMENT

This work was supported in part by the National Natural Science Foundation of China under Grant 51809030 and Grant 61871417, in part by the Natural Science Foundation of Liaoning Province under Grant 2020-MS-127, in part by the Liaoning Revitalization Talents Program under Grant XLYC2007067, and in part by the Fundamental Research Funds for the Central Universities under Grant 3132021231.

APPENDIX A.

According to the CLT-TL circuit shown in Figure 1(b), the $ABCD$ matrix $[\mathbf{M}_T]$ of the CLT-TL can be derived, as shown in Eq. (A1).

$$\begin{aligned}[\mathrm{M_T}] &= \begin{bmatrix} A_T & B_T \\ C_T & D_T \end{bmatrix} \\ &= \begin{bmatrix} A_2^3 + 3A_2B_2C_2 + Y_{o1}\left(3A_2^2B_2 + B_2^2C_2\right) & 3A_2^2B_2 + B_2^2C_2 \\ 2Y_{o1}\left(A_2^3 + 3A_2B_2C_2\right) + Y_{o1}^2\left(3A_2^2B_2 + B_2^2C_2\right) + 3A_2^2C_2 + B_2C_2^2 & A_2^3 + 3A_2B_2C_2 + Y_{o1}\left(3A_2^2B_2 + B_2^2C_2\right) \end{bmatrix}\end{aligned} \tag{A1}$$

where

$$A_2 = \cos 2\theta_1 - \frac{Z_1}{2Z_2}\sin 2\theta_1 \tan\theta_2 \tag{A2}$$

$$B_2 = \mathrm{j}\cdot Z_1 \cdot \sin 2\theta_1 - \mathrm{j}\cdot\frac{Z_1^2}{Z_2}\sin^2\theta_1 \tan\theta_2 \tag{A3}$$

$$C_2 = \frac{\mathrm{j}}{Z_1}\sin 2\theta_1 + \frac{\mathrm{j}}{Z_2}\cos^2\theta_1 \tan\theta_2 \tag{A4}$$

$$Y_{o1} = \mathrm{j}\frac{\dfrac{1}{Z_o}\tan\theta_o + \omega C}{1 - Z_o\omega C\tan\theta_o} - \mathrm{j}\frac{1 - \dfrac{1}{Z_o}\omega L\tan\theta_o}{\omega L + Z_o\tan\theta_o} \tag{A5}$$

For the two-end short-circuited coupled lines in Figure 1 (1c), the $ABCD$ matrix $[\mathbf{M}_S]$ can be expressed in the following according to [18].

$$\begin{aligned}[\mathrm{M_S}] &= \begin{bmatrix} A_s & B_s \\ C_s & D_s \end{bmatrix} \\ &= \begin{bmatrix} \dfrac{\cot\theta_\mathrm{c}/Z_{0e} + \cot\theta_\mathrm{c}/Z_{0o}}{\csc\theta_\mathrm{c}/Z_{0e} - \csc\theta_\mathrm{c}/Z_{0o}} & \dfrac{2\mathrm{j}}{\csc\theta_\mathrm{c}/Z_{0e} - \csc\theta_\mathrm{c}/Z_{0o}} \\ \dfrac{\mathrm{j}}{2}\cdot\dfrac{1/Z_{0e}^2 + 1/Z_{0o}^2 - 2\left(\cot^2\theta_\mathrm{c} + \csc^2\theta_\mathrm{c}\right)/(Z_{0e}Z_{0o})}{\csc\theta_\mathrm{c}/Z_{0e} - \csc\theta_c/Z_{0o}} & \dfrac{\cot\theta_\mathrm{c}/Z_{0e} + \cot\theta_\mathrm{c}/Z_{0o}}{\csc\theta_\mathrm{c}/Z_{0e} - \csc\theta_\mathrm{c}/Z_{0o}} \end{bmatrix}\end{aligned} \tag{A6}$$

Then, the $ABCD$ parameters (A_c, B_c, C_c, D_c) of the SLS-CL in Figure 1(c) can be derived by multiplying the matrix of two-end short-circuited coupled lines with that of the open-stub loaded transmission lines. Equations (A7)–(A9) shows the derived expressions.

$$A_C = D_C = \begin{bmatrix} \left(\cos 2\theta_3 - \dfrac{Z_3}{Z_4}\sin 2\theta_3 \tan\theta_4\right)\left(\dfrac{\cot\theta_c/Z_{0e} + \cot\theta_c/Z_{0o}}{\csc\theta_c/Z_{0e} - \csc\theta_c/Z_{0o}}\right) \\ -\left(\cos\theta_3 - \dfrac{Z_3}{Z_4}\tan\theta_4\sin\theta_3\right)\left(\dfrac{\sin\theta_3}{Z_3} + \dfrac{\cos\theta_3\tan\theta_4}{Z_4}\right)\left(\dfrac{2}{\csc\theta_c/Z_{0e} - \csc\theta_c/Z_{0o}}\right) \\ -\dfrac{Z_3\sin 2\theta_3}{4}\left(\dfrac{1/Z_{0e}^2 + 1/Z_{0o}^2 - 2\left(\cot^2\theta_c + \csc^2\theta_c\right)/(Z_{0e}Z_{0o})}{\csc\theta_c/Z_{0e} - \csc\theta_c/Z_{0o}}\right) \end{bmatrix} \quad \text{(A7)}$$

$$B_C = j\begin{bmatrix} Z_3\left(\sin 2\theta_3 - \dfrac{2}{Z_4}\tan\theta_4\sin^2\theta_3\right)\left(\dfrac{\cot\theta_c/Z_{0e} + \cot\theta_c/Z_{0o}}{\csc\theta_c/Z_{0e} - \csc\theta_c/Z_{0o}}\right) \\ +\dfrac{2\left(\cos\theta_3 - \dfrac{Z_3}{Z_4}\tan\theta_4\sin\theta_3\right)^2}{\csc\theta_c/Z_{0e} - \csc\theta_c/Z_{0o}} - \dfrac{Z_3^2\sin^2\theta_3}{2}\cdot\dfrac{1/Z_{0e}^2 + 1/Z_{0o}^2 - 2\left(\cot^2\theta_c + \csc^2\theta_c\right)/(Z_{0e}Z_{0o})}{\csc\theta_c/Z_{0e} - \csc\theta_c/Z_{0o}} \end{bmatrix} \quad \text{(A8)}$$

$$C_C = j\begin{bmatrix} \left(\dfrac{\sin 2\theta_3}{Z_3} + \dfrac{2\tan\theta_4\cos^2\theta_3}{Z_4}\right)\left(\dfrac{\cot\theta_c/Z_{0e} + \cot\theta_c/Z_{0o}}{\csc\theta_c/Z_{0e} - \csc\theta_c/Z_{0o}}\right) \\ -\dfrac{2\left(\dfrac{\sin\theta_3}{Z_3} + \dfrac{\cos\theta_3\tan\theta_4}{Z_4}\right)^2}{\csc\theta_c/Z_{0e} - \csc\theta_c/Z_{0o}} + \dfrac{\cos^2\theta_3}{2}\cdot\dfrac{1/Z_{0e}^2 + 1/Z_{0o}^2 - 2\left(\cot^2\theta_c + \csc^2\theta_c\right)/(Z_{0e}Z_{0o})}{\csc\theta_c/Z_{0e} - \csc\theta_c/Z_{0o}} \end{bmatrix} \quad \text{(A9)}$$

REFERENCES

1. Pozar, D. M., *Microwave Engineering*, 3rd Edition, Wiley, New York, 2005.
2. Chang, W. S., C. H. Liang, and C. Y. Chang, "Slow-wave broadside-coupled microstrip lines and its application to the rat-race coupler," *IEEE Microw. Wireless Compon. Lett.*, Vol. 25, No. 6, 361–363, Jun. 2015.
3. Chang, E. S. and C. Y. Chang, "A high slow-wave factor microstrip structure with simple design formulas and its application to microwave circuit design," *IEEE Trans. Microw. Theory Techn.*, Vol. 60, No. 11, 3376–3383, Nov. 2012.
4. Wang, C. C., H. C. Chiu, and T. G. Ma, "A slow-wave multilayer synthesized coplanar waveguide and its applications to rat-race coupler and dual-mode filter," *IEEE Trans. Microw. Theory Techn.*, Vol. 59, No. 7, 1719–1729, Jul. 2011.
5. Wang, Y. Q., K. X. Ma, N. N. Yan, and L. Y. Li, "A slow-wave rat-race coupler using substrate integrated suspended line technology," *IEEE Trans. Compon. Packag. Manuf. Technol.*, Vol. 7, No. 4, 630–636, Apr. 2017.
6. Tseng, C. H. and H. J. Chen, "Compact rat-race coupler using shunt-stub-based artificial transmission lines," *IEEE Microw. Wireless Compon. Lett.*, Vol. 18, No. 11, 734–736, Nov. 2008.
7. Tseng, C. H. and C. L. Chang, "A rigorous design methodology for compact planar branch-line and rat-race couplers with asymmetrical T-structures," *IEEE Trans. Microw. Theory Techn.*, Vol. 60, No. 7, 2085–2092, Jul. 2012.
8. Okabe, H., C. Caloz, and T. Itoh, "A compact enhanced-bandwidth hybrid ring using an artificial lumped-element left-handed transmission-line section," *IEEE Trans. Microw. Theory Techn.*, Vol. 52, No. 3, 798–804, Mar. 2004.
9. Eccleston, K. W. and S. H. M. Ong, "Compact planar microstripline branch-line and rat-race couplers," *IEEE Trans. Microw. Theory Techn.*, Vol. 51, No. 10, 2119–2125, Oct. 2003.

10. Gu, J. and X. Sun, "Miniaturization and harmonic suppression of branch-line and rat-race hybrid coupler using compensated spiral compact microstrip resonant cell," *IEEE MTT-S Int. Microw. Symp. Dig.*, 1211–1214, 2005.
11. Lee, H. S., K. Choi, and H. Y. Hwang, "A harmonic and size reduced ring hybrid using coupled lines," *IEEE Microw. Wireless Compon. Lett.*, Vol. 17, No. 4, 259–261, Apr. 2007.
12. Ahn, H.-R. and M. M. Tentzeris, "Compact and wideband General Coupled-line Ring Hybrids (GCRHS) for arbitrary circumferences and arbitrary power-division ratios," *IEEE Access*, Vol. 7, 33414–33423, 2019.
13. Ahn, H.-R. and M. M. Tentzeris, "A novel wideband compact microstrip coupled-line ring hybrid for arbitrarily high power-division ratios," *IEEE Trans. Circuits Syst. II, Exp. Briefs*, Vol. 64, No. 6, 630–634, Jun. 2017.
14. Ahn, H. R. and S. Nam, "Wideband microstrip coupled-line ring hybrids for high power-division ratios," *IEEE Trans. Microw. Theory Techn.*, Vol. 61, No. 5, 1768–1780, May 2013.
15. Liang, C. H., W. S. Chang, and C. Y. Chang, "Enhanced coupling structures for tight couplers and wideband filters," *IEEE Trans. Microw. Theory Techn.*, Vol. 59, No. 3, 574–583, Oct. 2011.
16. Yeung, L. K. and Y. E. Wang, "A novel 180 hybrid using broadside-coupled asymmetric coplanar striplines," *IEEE Trans. Microw. Theory Techn.*, Vol. 55, No. 12, 2625–2630, Dec. 2007.
17. Pan, Y. F., S. Y. Zheng, Y. M. Pan, Y. X. Li, and Y. L. Long, "A frequency tunable quadrature coupler with wide tuning range of center frequency and wide operating bandwidth," *IEEE Trans. Circuits Syst. II, Exp. Briefs*, Vol. 65, No. 7, 864–868, Jul. 2018.
18. Zysman, G. I. and A. K. Johnson, "Coupled transmission line networks in an inhomogeneous dielectric medium," *IEEE Trans. Microw. Theory Techn.*, Vol. 17, No. 10, 753–759, Oct. 1969.
19. Muraguchi, M., T. Yukitake, and Y. Naito, "Optimum design of 3-dB branch-line couplers using microstrip lines," *IEEE Trans. Microw. Theory Techn.*, Vol. 31, No. 8, 674–678, 1983.
20. Kennedy, J. and R. Eberhart, "Particle swarm optimization," *ICNN95 — International Conference on Neural Networks*, 2002.